Journal of Computational Dynamics
doi:10.3934/jcd.2021022

APPLYING SPLITTING METHODS WITH COMPLEX COEFFICIENTS TO THE NUMERICAL INTEGRATION OF UNITARY PROBLEMS

Sergio Blanes*

Universitat Politècnica de València
Instituto de Matemática Multidisciplinar
46022-Valencia, Spain

Fernando Casas

Departament de Matemàtiques and IMAC
Universitat Jaume I
12071-Castellón, Spain

Alejandro Escorihuela-Tomàs

Departament de Matemàtiques
Universitat Jaume I
12071-Castellón, Spain

Abstract. We explore the applicability of splitting methods involving complex coefficients to solve numerically the time-dependent Schrödinger equation. We prove that a particular class of integrators are conjugate to unitary methods for sufficiently small step sizes when applied to problems defined in the group SU(2). In the general case, the error in both the energy and the norm of the numerical approximation provided by these methods does not possess a secular component over long time intervals, when combined with pseudo-spectral discretization techniques in space.

1. **Introduction.** Splitting methods constitute a natural choice for the numerical time integration of differential equations of the form

$$\frac{du}{dt} = A(u) + B(u), \qquad u(0) = u_0, \tag{1}$$

when each subproblem

$$\frac{du}{dt} = A(u), \qquad \frac{du}{dt} = B(u)$$

with $u(0) = u_0$ can be solved explicitly [3, 15, 19]. Then, by composing the solution of each part with appropriately chosen coefficients, it is possible to construct an

2020 *Mathematics Subject Classification.* Primary: 65L05, 37M15; Secondary: 65P10, 65M22.
Key words and phrases. Splitting methods, unitary problems, complex coefficients, preservation properties.
Work supported by Ministerio de Ciencia e Innovación (Spain) through project PID2019-104927GB-C21/AEI/10.13039/501100011033. A.E.-T. has been additionally funded by the predoctoral contract BES-2017-079697 (Spain).
*Corresponding author: Sergio Blanes.

integrator of a given order $r \geq 1$ for (1). In the particular case of a linear problem,

$$\frac{du}{dt} = Au + Bu, \tag{2}$$

a splitting method is a composition of the form

$$\Psi^{[r]}(h) = \mathrm{e}^{b_{s+1}hB}\mathrm{e}^{a_s hA}\mathrm{e}^{b_s hB}\cdots \mathrm{e}^{a_1 hA}\,\mathrm{e}^{b_1 hB}, \tag{3}$$

where $h := \Delta t$ is the time step and the coefficients a_j, b_j are chosen as solutions of the order conditions, a set of polynomial equations that must be satisfied to achieve an order of accuracy r, i.e., so that $\exp(h(A+B))u_0 - \Psi^{[r]}(h)u_0 = \mathcal{O}(h^{r+1})$.

The simplest example within this class is the Lie–Trotter splitting,

$$\mathrm{e}^{hA}\,\mathrm{e}^{hB} \qquad \text{or} \qquad \mathrm{e}^{hB}\,\mathrm{e}^{hA}, \tag{4}$$

providing a first order approximation ($r = 1$), whereas the palindromic versions

$$\mathcal{S}(h) = \mathrm{e}^{h/2A}\,\mathrm{e}^{hB}\,\mathrm{e}^{h/2A} \qquad \text{or} \qquad \mathcal{S}(h) = \mathrm{e}^{h/2B}\,\mathrm{e}^{hA}\,\mathrm{e}^{h/2B}, \tag{5}$$

known as Strang splittings, are methods of order $r = 2$.

Although very efficient high order splitting methods can be found in the literature for the numerical integration of Eq. (1), it is important to remark that if the order $r \geq 3$, then necessarily some of the coefficient a_j and b_j have to be negative [2, 21, 22]. This, while does not constitute a particular problem when the differential equation is reversible, makes unfeasible their application in parabolic differential equations of evolutionary type, when the operators A and B are only assumed to generate C^0 semi-groups (and not groups): in that case the flows e^{tA} and/or e^{tB} may not be defined for $t < 0$ [10, 16, 17]. Notice that this is the case, in particular, if A is the Laplacian operator.

Moreover, even in problems where splitting methods of order $r \geq 3$ can be safely applied, the presence of negative coefficients usually leads to large truncation errors, so that more stages than strictly necessary to achieve a given order have to be included in the composition to reduce these errors and improve the overall efficiency [6].

It is with the aim of circumventing these drawbacks that splitting methods with complex coefficients (with positive real part) have entered into the literature, mainly in the context of the integration of parabolic differential equations [10, 17, 5], but also for ordinary differential equations (ODEs) when structure-preserving (symplecticity, energy conservation, reversibility) is at stake [11].

Splitting and composition methods with complex coefficients, although computationally between 2 and 4 times more costly than their real counterparts when applied to ODEs involving real vector fields, possess however some remarkable properties: their truncation errors with the minimum number of stages are typically very small, and their stability threshold is comparatively large. Moreover, when the numerical solution is projected at each time step, they lead to approximations that still preserve important qualitative features (such as symplecticity and time-symmetry) up to an order much higher than the order of the method itself [7, 9, 4].

To better illustrate these points, let us consider a time-symmetric second order method $\mathcal{S}(h)$ (such as one of the compositions (5)). Then, a fourth-order method can be obtained by composition. More specifically, since the coefficients of such a scheme have to satisfy three order conditions, it makes sense to take three maps,

$$\mathcal{S}(\gamma_3 h)\,\mathcal{S}(\gamma_2 h)\,\mathcal{S}(\gamma_1 h).$$

In that case, the order conditions read [6, 15]

$$\sum_{j=1}^{3}\gamma_j = 1, \qquad \sum_{j=1}^{3}\gamma_j^3 = 0, \qquad \sum_{j=1}^{2}\left(\gamma_j^3\left(\sum_{k=j+1}^{3}\gamma_k\right) - \gamma_j\left(\sum_{k=j+1}^{3}\gamma_k^3\right)\right) = 0. \quad (6)$$

and admit only one real solution, namely

$$\gamma_1 = \gamma_3 = \frac{1}{2 - 2^{1/3}}, \qquad \gamma_2 = 1 - 2\gamma_1$$

leading to a time-symmetric composition scheme, usually referred to as Yoshida's method, here denoted as $\mathcal{S}^{[4]}(h)$. Notice, however, that there are four more complex solutions. The first pair,

$$\gamma_1 = \gamma_3 \equiv \gamma = \frac{1}{2 - 2^{1/3}\mathrm{e}^{2ik\pi/3}}, \qquad \gamma_2 = 1 - 2\gamma, \qquad k = 1, 2 \quad (7)$$

leads again to two time-symmetric methods, denoted as $\Psi^{[4]}_{P,c}(h)$, whereas the second one, denoted as $\Psi^{[4]}_{SC,c}(h)$,

$$\gamma_1 = \bar{\gamma}_3 = \frac{1}{4} \pm i\,\frac{1}{4}\sqrt{\frac{5}{3}}, \qquad \gamma_2 = \frac{1}{2} \quad (8)$$

(here the bar indicates the complex conjugate), corresponds to a so–called *symmetric-conjugate* composition method [4]: it is symmetric in the real part of the coefficients and skew-symmetric in the imaginary part. Here and in the sequel, the first sub-index in a method (either P or SC) refers to its type (either palindromic or symmetric-conjugate, respectively), whereas the second sub-index (either r or c) indicates that the a_i coefficients in the splitting are real or complex, respectively.

At order five there are two additional order conditions. One of them, $\omega_{5,1} = \sum_{j=1}^{3}\gamma_j^5$, has been typically used to measure the relative error of methods of the same class. If one defines the error as $\mathcal{E} = |\omega_{5,1}|$, then one has for the previous methods the following values of $\mathcal{E}$:

$$\begin{array}{ll} \mathcal{S}^{[4]}(h) & \mathcal{E} = 5.29\ldots, \\ \Psi^{[4]}_{P,c}(h) & \mathcal{E} = 0.024\ldots, \\ \Psi^{[4]}_{SC,c}(h) & \mathcal{E} = 0.027\ldots \end{array}$$

Notice that the error of methods with complex coefficients is about 200 smaller than in the real case.

In the particular case in which $\mathcal{S}(h)$ is given by (5), the previous methods can also be written as

$$\mathrm{e}^{b_4 hB}\,\mathrm{e}^{a_3 hA}\,\mathrm{e}^{b_3 hB}\,\mathrm{e}^{a_2 hA}\,\mathrm{e}^{b_2 hB}\,\mathrm{e}^{a_1 hA}\,\mathrm{e}^{b_1 hB}, \quad (9)$$

with

$$b_1 = \frac{1}{2}\gamma_1, \quad a_1 = \gamma_1, \quad b_2 = \frac{1}{2}(\gamma_1 + \gamma_2), \quad a_2 = \gamma_2,$$
$$b_3 = \frac{1}{2}(\gamma_2 + \gamma_3), \quad a_3 = \gamma_3, \quad b_4 = \frac{1}{2}\gamma_3.$$

As a matter of fact, the simplest symmetric-conjugate composition corresponds to the third order scheme

$$\Psi^{[3]}_{SC,c}(h) = \mathcal{S}^{[2]}_{\alpha_2 h} \circ \mathcal{S}^{[2]}_{\alpha_1 h}, \quad (10)$$

with

$$\alpha_1 = \bar{\alpha}_2 \equiv \alpha = \frac{1}{2} + i\frac{\sqrt{3}}{6}.$$

For equation (2), method (10) can be written as

$$\Psi^{[3]}_{SC,c}(h) = \mathrm{e}^{\bar{b}_1 hB}\, \mathrm{e}^{\bar{a}_1 hA}\, \mathrm{e}^{b_2 hB}\, \mathrm{e}^{a_1 hA}\, \mathrm{e}^{b_1 hB}, \tag{11}$$

with $a_1 = \alpha$, $b_1 = \alpha/2$, $b_2 = 1/2$.

Although (11) is of order 3, if A and B are real, then it renders a scheme of order 4 when it is projected on the real axis after each time step. In addition, it verifies $\Psi^{[3]}_{SC,c}(-h) \circ \Psi^{[3]}_{SC,c}(h) = I + \mathcal{O}(h^8)$. It is said that the scheme is pseudo-symmetric of order 7, since it preserves the time-symmetry property up to terms of order h^7 [9].

Schemes with complex coefficients have been proposed before for the treatment of quantum problems, mainly in the context of imaginary time propagation, with the purpose of computing ground state energies [1] and in quantum Monte Carlo simulations [23, 14], but also in the decomposition of unitary operators [20]. In the later case it is shown, both for unitary 2×2 matrices and empirically for exponentials of Gaussian random Hermitian matrices, that a splitting method does indeed possess a maximal time step for which the scheme is numerically stable. We generalize the treatment to differential equations defined in SU(2) for methods possessing a particular symmetry and eventually examine their behavior when they are applied to the time dependent Schrödinger equation.

2. Splitting methods in SU(2).

In the study of the evolution of two-level quantum systems one has to deal with the Schrödinger equation, which in this context reads ($\hbar = 1$)

$$i\frac{dU}{dt} = H\,U, \qquad U(0) = I, \tag{12}$$

where $U(t)$ is a 2×2 unitary matrix with unit determinant and the skew-Hermitian Hamiltonian H can be expressed as a linear combination of Pauli matrices,

$$\sigma_1 = \begin{pmatrix} 0 & 1 \\ 1 & 0 \end{pmatrix}, \qquad \sigma_2 = \begin{pmatrix} 0 & -i \\ i & 0 \end{pmatrix}, \qquad \sigma_3 = \begin{pmatrix} 1 & 0 \\ 0 & -1 \end{pmatrix}. \tag{13}$$

Since our purpose is to analyze splitting methods in this context, we assume that H can be written as

$$H = \mathbf{a}\cdot\sigma + \mathbf{b}\cdot\sigma \tag{14}$$

for given vectors $\mathbf{a}, \mathbf{b} \in \mathbb{R}^3$ and $\sigma = (\sigma_1, \sigma_2, \sigma_3)$, so that, by comparing with (2), one has $A \equiv -i\,\mathbf{a}\cdot\sigma$ and $B \equiv -i\,\mathbf{b}\cdot\sigma$. The exact solution of Eq. (12) after one time step h is

$$U_{\mathrm{ex}}(h) = \mathrm{e}^{-ihH} = \mathrm{e}^{-ih(\mathbf{a}\cdot\sigma + \mathbf{b}\cdot\sigma)}.$$

On the other hand, if a splitting method of the form (3) of order r with *real* coefficients is applied to solve this very simple problem, it is clear that the corresponding approximation can be written as

$$U_{\mathrm{app}}(h) = \mathrm{e}^{-i\,h\,\mathbf{d}(h)\cdot\sigma}, \qquad \text{where} \qquad \mathbf{d}(h) = \mathbf{a} + \mathbf{b} + \mathcal{O}(h^r) \in \mathbb{R}^3,$$

and thus the method still renders an approximation in SU(2). The situation is different, however, when the splitting method (3) involves *complex* coefficients, since in that case $\mathbf{d}(h) \in \mathbb{C}^3$ and the approximation is no longer unitary. In general, the scheme will be unstable and the errors will grow exponentially along the integration.

Example. At this point it is worth testing the previous third- and fourth-order schemes obtained by composing the Strang splitting and involving complex coefficients, namely $\Psi^{[3]}_{SC,c}(h)$, $\Psi^{[4]}_{SC,c}(h)$, and $\Psi^{[4]}_{P,c}(h)$. To do that, we consider the following simple Hamiltonian in SU(2): $H = \sigma_1 + \sigma_2$, or alternatively, $\mathbf{a} = (1, 0, 0)$, $\mathbf{b} = (0, 1, 0)$ in (14).

In our experiment, we take as initial condition $U(t_0 = 0) = I$, integrate Eq. (12) with different values of the time step h and compute the error of the approximation (in the 2-norm) at the final time $t_f = 10$ as a function of the computational cost (estimated as the number of exponentials involved in the whole integration). The results obtained with each method are displayed in Figure 1 (left panel). We notice that all schemes involving complex coefficients provide considerably more accurate results than $\mathcal{S}^{[4]}(h)$ (black solid line), the fourth-order methods being also more efficient than $\Psi^{[3]}_{SC,c}(h)$ for high accuracy.

In order to check how each scheme with complex coefficients behaves with respect to unitarity, we take as a final time $t_f = 1000$, and adjust h (and therefore the number of iterations N) so that they require the same computational cost. Specifically, $N = 6000$ ($h = 1/6$) for scheme $\Psi^{[3]}_{SC,c}(h)$ and $N = 4000$ ($h = 1/4$) for all methods of order 4. Finally we compute $|\|U_{\rm app}(nh)\| - 1|$, $n = 1, 2, \ldots, N = (t_f - t_0)/h$, where $U_{\rm app}(nh)$ denotes the approximate solution after n steps. The outcome is depicted in Figure 1 (right panel). Notice how the error in unitarity grows for $\Psi^{[4]}_{P,c}(h)$, whereas it is bounded, even for large intervals, for the symmetric-conjugate methods $\Psi^{[3]}_{SC,c}(h)$ and $\Psi^{[4]}_{SC,c}(h)$. Among them, the later clearly provides more accurate results.

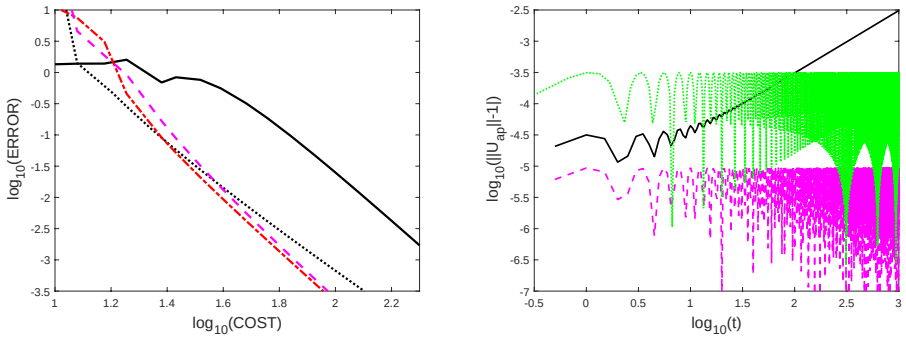

FIGURE 1. Left: 2-norm error vs. computational cost (number of exponentials) for $\Psi^{[3]}_{SC,c}$ (dotted line), $\mathcal{S}^{[4]}$ (real coefficients, solid line), $\Psi^{[4]}_{P,c}$ (complex coefficients, dash-dotted line) and $\Psi^{[4]}_{SC,c}$ (dashed line). Right: Error in unitarity for $\Psi^{[4]}_{P,c}$ (solid line) and the symmetric-conjugate methods $\Psi^{[3]}_{SC,c}$ (dotted line) and $\Psi^{[4]}_{SC,c}$ (dashed line).

This marked difference of both types of integrators can also be illustrated by computing the eigenvalues λ_1, λ_2 of the approximate solution after one step size, i.e., of the corresponding matrix $U_{\rm app}(h)$. In the exact case, of course, both evolve on the unit circle in the complex plane, whereas here one has still $\lambda_1\lambda_2 = 1$, since the determinant is one. In Figure 2 we depict $|\lambda_j|$, $j = 1, 2$, as a function of h for

the palindromic scheme $\Psi^{[4]}_{P,c}$ with $k = 1$ (black, dashed lines) and the symmetric-conjugate splittings $\Psi^{[3]}_{SC,c}$ (blue, dotted line) and $\Psi^{[4]}_{SC,c}$ (red, solid line) in the range $1 \leq h \leq 3$. It is worth remarking that for the symmetric-conjugate methods both $|\lambda_j|$ are exactly 1 for $0 \leq h \leq h^*$, with $h^* = 1.7570473$ for $\Psi^{[3]}_{SC,c}$ and $h^* = 2.9139468357$ for $\Psi^{[4]}_{SC,c}$. In other words, they behave as unitary maps when $h \leq h^*$. On the other hand, it can be checked that $|\lambda_1| > 1$ for any $h > 0$ for $\Psi^{[4]}_{P,c}$. □

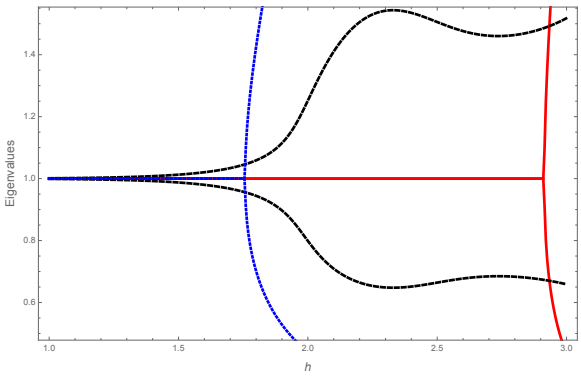

FIGURE 2. Absolute value of the eigenvalues of the approximate solution matrix obtained with $\Psi^{[4]}_{P,c}$ with complex coefficients ($k = 1$, black dashed line), $\Psi^{[3]}_{SC,c}$ (blue dotted line) and $\Psi^{[4]}_{SC,c}$ (red, solid line).

The previous example illustrates in fact a general pattern exhibited by symmetric-conjugate methods for this problem, as we next prove.

Proposition 1. *Suppose a symmetric-conjugate splitting method of the form (3), with $a_{s+1-j} = \bar{a}_j$, $b_{s+2-j} = \bar{b}_j$, is applied to the numerical integration of the Schrödinger equation (12) with the Hamiltonian given by (14). In that case, the following statements hold:*

(a) The eigenvalues of the matrix approximating the solution after one time step h lie on the unit circle in the complex plane for sufficiently small h.

(b) The symmetric-conjugate splitting method is itself conjugate to a unitary method for sufficiently small h.

Proof. When a splitting method of the form (3) is applied to solve Eq. (12), the corresponding approximation after one step can be written as $U_{\text{app}}(h) = \exp(V(h))$, where $V(h)$ is a linear combination of A, B and all their nested commutators,

$$V(h) = h(w_{1,1}A + w_{1,2}B) + h^2 w_{2,1}[A,B] + h^3(w_{3,1}[A,[A,B]] + w_{3,2}[B,[A,B]]) + \mathcal{O}(h^4), \tag{15}$$

and $w_{n,k}$ are polynomials in the coefficients a_j, b_j. Method (3) is of order r if $w_{1,1} = w_{1,2} = 1$ and the polynomials $w_{n,k}$ vanish for $1 < n < r$. In our case, since

$$[-i\,\mathbf{a}\cdot\sigma, -i\,\mathbf{b}\cdot\sigma] = -i\,2\,(\mathbf{a}\times\mathbf{b})\cdot\sigma,$$

it is clear that the vector fields associated with all commutators in (15) containing an even number of operators are perpendicular to the plane generated by the vectors $\mathbf{a}$ and $\mathbf{b}$, whereas those containing an odd number of operators A and B are in such

a plane. If in addition the method is symmetric-conjugate, then a straightforward computation shows that $V^\dagger(h) = V(-h)$, and so all polynomials $w_{2j+1,k}$ are real whereas all polynomials $w_{2j,k}$ are pure imaginary. Therefore, $V(h)$ can be written as

$$V(h) = -i\,h\tilde{H}(h), \qquad \text{with} \qquad \tilde{H}(h) = \mathbf{d}(h)\cdot\sigma + i\,\mathbf{c}(h)\cdot\sigma, \tag{16}$$

for two vectors $\mathbf{c}, \mathbf{d} \in \mathbb{R}^3$ verifying $\mathbf{c}\cdot\mathbf{d} = 0$ and

$$\mathbf{d}(h) = \mathbf{a} + \mathbf{b} + \mathcal{O}(h^{r+1}), \qquad \mathbf{c}(h) = \mathcal{O}(h^r). \tag{17}$$

This special structure of $\tilde{H}(h)$ allows one to obtain statements (a) and (b) above. First, if we write

$$\mathrm{e}^{-i\,h\tilde{H}(h)} = \mathrm{e}^{h\,\mathbf{u}\cdot\sigma}, \qquad \text{with} \qquad \mathbf{u} = \mathbf{c} - i\,\mathbf{d},$$

then

$$U_{\rm app}(h) = \mathrm{e}^{h\,\mathbf{u}\cdot\sigma} = \cosh(hu)I + \frac{\sinh(hu)}{u}\,\mathbf{u}\cdot\sigma,$$

with $u = \sqrt{\mathbf{u}\cdot\mathbf{u}} = (\|\mathbf{c}\|^2 - \|\mathbf{d}\|^2)^{1/2}$. Of course, if $\|\mathbf{c}\| < \|\mathbf{d}\|$, then $\cosh(u) = \cos\alpha$, $\sinh(u) = i\sin\alpha$, with $\alpha = (\|\mathbf{d}\|^2 - \|\mathbf{c}\|^2)^{1/2}$, and the eigenvalues of $U_{\rm app}(h)$ are $\lambda_{1,2} = \exp(\pm ih\alpha(h))$. But, in virtue of (17), this always holds for sufficiently small values of h.

Statement (b) can demonstrated as follows. Let us introduce the unitary vector

$$\mathbf{C} = \frac{\mathbf{d}\times\mathbf{c}}{\|\mathbf{d}\times\mathbf{c}\|}.$$

A trivial computation shows that

$$\mathbf{d}\times\mathbf{C} = -\frac{\|\mathbf{d}\|}{\|\mathbf{c}\|}\,\mathbf{c}, \qquad \mathbf{c}\times\mathbf{C} = \frac{\|\mathbf{c}\|}{\|\mathbf{d}\|}\,\mathbf{d},$$

and furthermore, for a given parameter $s \in \mathbb{R}$,

$$\mathrm{e}^{s\,\mathbf{C}\cdot\sigma}\,\mathrm{e}^{h\mathbf{u}\cdot\sigma}\,\mathrm{e}^{-s\,\mathbf{C}\cdot\sigma} = \exp\left(\mathrm{e}^{s\,\mathbf{C}\cdot\sigma}\,(h\,\mathbf{u}\cdot\sigma)\,\mathrm{e}^{-s\,\mathbf{C}\cdot\sigma}\right).$$

From the definition of $\mathbf{C}$ and the properties of the Pauli matrices [13], one has

$$\begin{aligned}
\mathrm{e}^{s\,\mathbf{C}\cdot\sigma}\,(\mathbf{c}\cdot\sigma)\,\mathrm{e}^{-s\,\mathbf{C}\cdot\sigma} &= \cosh(2s)(\mathbf{c}\cdot\sigma) - i\,\sinh(2s)\frac{\|\mathbf{c}\|}{\|\mathbf{d}\|}\,\mathbf{d}\cdot\sigma \\
\mathrm{e}^{s\,\mathbf{C}\cdot\sigma}\,(\mathbf{d}\cdot\sigma)\,\mathrm{e}^{-s\,\mathbf{C}\cdot\sigma} &= \cosh(2s)(\mathbf{d}\cdot\sigma) + i\,\sinh(2s)\frac{\|\mathbf{d}\|}{\|\mathbf{c}\|}\,\mathbf{c}\cdot\sigma,
\end{aligned}$$

and thus

$$\begin{aligned}
&\mathrm{e}^{s\,\mathbf{C}\cdot\sigma}\,(\mathbf{u}\cdot\sigma)\,\mathrm{e}^{-s\,\mathbf{C}\cdot\sigma} = \\
&\qquad\left(\sinh(2s)\frac{\|\mathbf{d}\|}{\|\mathbf{c}\|} + \cosh(2s)\right)\mathbf{c}\cdot\sigma - i\left(\sinh(2s)\frac{\|\mathbf{c}\|}{\|\mathbf{d}\|} + \cosh(2s)\right)\mathbf{d}\cdot\sigma.
\end{aligned}$$

If we now take s such that

$$\sinh(2s)\frac{\|\mathbf{d}\|}{\|\mathbf{c}\|} + \cosh(2s) = 0, \qquad \text{i.e.,} \qquad \tanh(2s) = -\frac{\|\mathbf{c}\|}{\|\mathbf{d}\|}, \tag{18}$$

then, clearly

$$\mathrm{e}^{s\,\mathbf{C}\cdot\sigma}\,(-ih\tilde{H})\,\mathrm{e}^{-s\,\mathbf{C}\cdot\sigma} = -i\,h\,\mathbf{D}(h)\cdot\sigma,$$

with

$$\mathbf{D}(h) = \sinh(2s)\left(\frac{\|\mathbf{c}\|}{\|\mathbf{d}\|} - \frac{\|\mathbf{d}\|}{\|\mathbf{c}\|}\right)\mathbf{d} \in \mathbb{R}^3.$$

In consequence,

$$\mathrm{e}^{s\,\mathbf{C}\cdot\sigma}\,\mathrm{e}^{-ih\tilde{H}}\,\mathrm{e}^{-s\,\mathbf{C}\cdot\sigma} = \mathrm{e}^{-ih\mathbf{D}(h)\cdot\sigma}. \tag{19}$$

In other words, if s is such that Eq. (18) holds, then the map obtained by applying a symmetric-conjugate splitting method is conjugate to a unitary matrix. Notice that if $\|\mathbf{c}\| < \|\mathbf{d}\|$ this is always possible, in agreement with statement (a) for the eigenvalues of the approximate solution matrix. □

Proposition 1 thus provides a rigorous justification of the results shown in Figures 1 and 2: since a symmetric-conjugate splitting method is ultimately conjugate to a unitary map in the sense of eq. (19) for sufficiently small values of h, then the error in the unitarity of the numerical solution is bounded, whereas the eigenvalues remain on the unit circle in the complex plane.

Methods of the form (19) are called *processed* or *corrected* in the literature (see, e.g. [3, 6, 15, 19]). In that context, method $\mathrm{e}^{-ih\tilde{H}}$ is called the kernel, and $\mathrm{e}^{s\,\mathbf{C}\cdot\sigma}$ the processor. For integrators of this class, only the error terms in the kernel that cannot be removed by a processor are relevant in the long run. In the case of unitary problems in SU(2) we have shown that any symmetric-conjugate splitting method is indeed the kernel of a processed unitary scheme.

3. **Application to the time-dependent Schrödinger equation.** In view of the previous results in SU(2), it is natural to examine the situation when splitting methods with complex coefficients, and in particular symmetric-conjugate schemes, are applied in a more general setting. To this end, we next consider the numerical integration of the general time dependent Schrödinger equation

$$i\frac{\partial}{\partial t}\psi(x,t) = -\frac{1}{2\mu}\Delta\psi(x,t) + V(x)\psi(x,t), \tag{20}$$

where now $\psi : \mathbb{R}^d \times \mathbb{R} \longrightarrow \mathbb{C}$ is the wave function representing the state of the system and the initial state is $\psi(x,0) = \psi_0(x)$. We take again $\hbar = 1$ and a reduced mass μ. Equation (20) can be written as

$$i\frac{\partial}{\partial t}\psi = (\hat{T}(P) + \hat{V}(X))\psi, \tag{21}$$

with $\hat{T}(P) = P^2/(2\mu)$, and the operators X and P are defined by their actions on $\psi(x,t)$ as

$$X\psi(x,t) = x\,\psi(x,t), \qquad P\;\psi(x,t) = -i\,\nabla\psi(x,t). \tag{22}$$

The usual procedure for applying splitting methods in this setting consists first in discretizing the space variables x, so as to get a system of ordinary differential equations (ODEs) which is subsequently integrated in time by the splitting scheme. If, for simplicity, we consider the one-dimensional problem, $d = 1$, and suppose that it is defined in $x \in [x_0, x_N]$, first this interval is partitioned into N parts of length $\Delta x = (x_N - x_0)/N$ and the vector $u = (u_0, \ldots, u_{N-1})^T \in \mathbb{C}^N$ is formed, with $u_n = \psi(x_n, t)$ and $x_n = x_0 + n\Delta x$, $n = 0, 1, \ldots, N-1$. The partial differential equation (20) is then replaced by the N-dimensional linear ODE

$$i\frac{d}{dt}u(t) = H\,u(t), \qquad u(0) = u_0 \in \mathbb{C}^N, \tag{23}$$

where now H represents the (real symmetric) $N \times N$ matrix associated with the Hamiltonian.

When a Fourier spectral collocation method is used, then the matrix H in (23) is

$$H = T + V, \tag{24}$$

where V is a diagonal matrix associated with the potential $\hat{V}$ and T is a (full) differentiation matrix related with the kinetic energy $\hat{T}$. Their action on the wave function vector u is trivial: on the one hand, $(Vu)_n = V(x_n)u_n$ and thus the product Vu requires to compute N complex multiplications. On the other hand, $Tu = \mathcal{F}^{-1} D_T \mathcal{F} u$, where $\mathcal{F}$ and $\mathcal{F}^{-1}$ are the forward and backward discrete Fourier transform, and D_T is again diagonal. The transformation $\mathcal{F}$ from the discrete coordinate representation to the discrete momentum representation (and back) is done via the fast Fourier transform (FFT) algorithm, requiring $\mathcal{O}(N \log N)$ operations.

Notice that, since

$$\left(\mathrm{e}^{\tau V} u\right)_i = \mathrm{e}^{\tau V(x_i)} u_i, \qquad \mathrm{e}^{\tau T} u = \mathcal{F}^{-1} \mathrm{e}^{\tau D_T} \mathcal{F}\, u,$$

splitting methods constitute a valid alternative to approximate the solution $u(t) = \mathrm{e}^{\tau(T+V)} u_0$ for a time step Δt, with $\tau = -i\Delta t$. Thus, with the Lie–Trotter scheme (4) one has

$$\mathrm{e}^{\tau(T+V)} = \mathrm{e}^{\tau T}\, \mathrm{e}^{\tau V} + \mathcal{O}(\tau^2),$$

whereas the 2nd-order Strang splitting (5) constructs the numerical approximation u_{n+1} at time $t_{n+1} = t_n + \Delta t$ by

$$u_{n+1} = \mathrm{e}^{\tau/2V}\, \mathrm{e}^{\tau T}\, \mathrm{e}^{\tau/2V}\, u_n \equiv \mathcal{S}(\tau) u_n.$$

The resulting scheme is called split-step Fourier method in the chemical literature, and has some remarkable properties. In particular, it is both unitary and symplectic [18], as well as time-reversible. In addition, for suitable regularity assumptions on the potential and on the norm of the commutators $[\hat{T}, \hat{V}] = \hat{T}\hat{V} - \hat{V}\hat{T}$ and $[\hat{T}, [\hat{T}, \hat{V}]]$, the error at t_n is bounded by

$$\|u_n - u(t)\| \leq C\, \Delta t^2\, t \max_{0 \leq s \leq t} \|u(s)\|_2.$$

Higher order methods can be obtained of course by considering compositions (3), which in this setting read

$$\Psi^{[r]}(\tau) = \mathrm{e}^{b_{s+1}\tau V} \mathrm{e}^{a_s \tau T} \mathrm{e}^{b_s \tau V} \cdots \mathrm{e}^{a_1 \tau T}\, \mathrm{e}^{b_1 \tau V}, \tag{25}$$

and in fact, a large collection of practical schemes of different orders exist for carrying out the numerical integration (see e.g. [6, 15, 19] and references therein). In addition, from (22), it is clear that $[\hat{X}, \hat{P}]\ \psi(x,t) = i\, \psi(x,t)$, and so

$$[\hat{V}, [\hat{V}, [\hat{V}, \hat{T}]]]\ \psi(x,t) = 0. \tag{26}$$

This property leads to a reduction in the number of order conditions necessary to achieve a given order r and allows one to construct highly efficient schemes.

4. Splitting methods with complex coefficients.

When exploring the applicability of splitting methods with complex coefficients to the general time-dependent Schrödinger equation, several aspects must be addressed. First, since the computational cost of method (25) is dominated by the number of FFTs per step, the presence of complex a_j, b_j does not contribute significantly to increase this cost. In addition, it has been shown in other problems that splitting methods with complex coefficients involving the minimum number of flows to achieve a given order already provide good efficiency, in contrast with their real counterparts. On the other hand,

however, since $\sum_j a_j = 1$ for a consistent method, if $a_j \in \mathbb{C}$, then imaginary parts positive *and* negative enter into the game, with the result that severe instabilities may arise in practice due to the unboundedness of the Laplace operator. With respect to the potential, since in regions where it takes large values the wave function typically is close to zero, we can introduce an artificial cut-off bound in the computation if necessary, so that complex b_j can in principle be used, at least for a sufficiently small Δt. It makes sense therefore to construct and examine in detail methods with real a_j and complex b_j coefficients.

In the following, and for simplicity, we restrict ourselves to splitting methods (25) of order $r \leq 4$, which we denote by their sequence of coefficients as

$$(b_{s+1}, a_s, b_s, \ldots, a_2, b_2, a_1, b_1).$$

The order conditions are then

$$\begin{aligned}
&\text{Order 1:} && \sum_{i=1}^{s} a_i = 1, && \sum_{i=1}^{s} b_i = 1, \\
&\text{Order 2:} && \sum_{i=1}^{s} b_i \left(\sum_{j=1}^{i} a_j \right) = \frac{1}{2}, \\
&\text{Order 3:} && \sum_{i=1}^{s} b_i \left(\sum_{j=1}^{i} a_j \right)^2 = \frac{1}{3}, && \sum_{i=1}^{s} a_i \left(\sum_{j=i}^{s} b_j \right)^2 = \frac{1}{3}, \\
&\text{Order 4:} && \sum_{i=1}^{s} b_i \left(\sum_{j=1}^{i} a_j \right)^3 = \frac{1}{4}, && \sum_{i=1}^{s} a_i \left(\sum_{j=i}^{s} b_j \right)^3 = \frac{1}{4}, \\
& && \sum_{i=1}^{s} a_i^2 \left(\sum_{j=i}^{s} b_j \right)^2 + 2 \sum_{i=2}^{s} a_i \left(\sum_{j=1}^{i-1} a_j \right) \left(\sum_{k=i}^{s} b_k \right)^2 = \frac{1}{6}.
\end{aligned} \tag{27}$$

In typical applications of splitting methods with real coefficients, only palindromic sequences of coefficients, i.e., methods (25) with $b_{s+2-j} = b_j$, $a_{s+1-j} = a_j$ for all j are used. In that case, all the conditions at even order are automatically satisfied and the resulting schemes are time-symmetric, $\Psi^{[r]}(\tau)\, \Psi^{[r]}(-\tau) = I$, and of even order. Here, however, since we are dealing with complex coefficients, we also analyze the case $r = 3$ for completeness.

Order 3. The first five order conditions in (27) admit solutions with all a_j real and positive and $b_j \in \mathbb{C}$ with positive real part if one considers a composition of the form

$$\Psi^{[3]}_{SC,r}(\tau) = (\bar{b}_1, a_1, \bar{b}_2, a_2, b_2, a_1, b_1) \tag{28}$$

involving 6 parameters. Then one gets a 1-parametric family of solutions (+c.c.) with the required properties. Among them, we choose

$$a_1 = \frac{3}{10}, \qquad a_2 = \frac{2}{5}, \qquad b_1 = \frac{13}{126} - i\frac{\sqrt{59/2}}{63}, \qquad b_2 = \frac{25}{63} + i\frac{5\sqrt{59/2}}{126}.$$

Composition (11) constitutes of course another symmetric-conjugate method of order 3, denoted here by

$$\Psi^{[3]}_{SC,c}(\tau) = (\bar{b}_1, \bar{a}_1, b_2, a_1, b_1) \tag{29}$$

and involving less maps, although in this case $a_1 \in \mathbb{C}$.

Order 4. The simplest approach to construct a palindromic scheme with $a_j \in \mathbb{R}$ and $b_j \in \mathbb{C}$ consists in taking all the a_j equal. In that case, with $s = 4$, one has enough parameters to solve the required four order conditions (at odd orders). Only two solutions (complex conjugate to each other) are obtained, as shown in [10], thus resulting in the scheme

$$\Psi^{[4]}_{P,r}(\tau) = (b_1, a_1, b_2, a_2, b_3, a_2, b_2, a_1, b_1) \tag{30}$$

with

$$a_1 = a_2 = \frac{1}{4}, \qquad b_1 = \frac{1}{10} - i\frac{1}{30}, \qquad b_2 = \frac{4}{15} + i\frac{2}{15}, \qquad b_3 = \frac{4}{15} - i\frac{1}{5}.$$

Although more efficient schemes can be obtained if one allows for different a_j's [5], since we are interested here mainly in the qualitative behavior of the different methods, we limit ourselves to (30) as representative of palindromic splitting methods with real a_j's and complex b_j's, whereas we can take scheme (9)

$$\Psi^{[4]}_{P,c}(\tau) = (b_1, a_1, b_2, a_2, b_2, a_1, b_1), \tag{31}$$

as representative of palindromic methods with both $a_j \in \mathbb{C}$ and $b_j \in \mathbb{C}$.

Symmetric-conjugate splitting methods with real a_j's require at least $s = 5$ stages, in which case one has a free parameter. If we fix this as $a_1 = 1/8$, we get the scheme

$$\Psi^{[4]}_{SC,r}(\tau) = (\bar{b}_1, a_1, \bar{b}_2, a_2, \bar{b}_3, a_3, b_3, a_2, b_2, a_1, b_1) \tag{32}$$

with

$$\begin{aligned}
a_2 &= 0.23670501659941197298,\\
a_3 &= 0.27658996680117605403,\\
b_1 &= 0.03881396214419327198 - 0.045572109263923104872\, i,\\
b_2 &= 0.19047619047619047619 + 0.115462072300408741306\, i,\\
b_3 &= 0.27070984737961625182 - 0.148322245509626403888\, i
\end{aligned}$$

It is worth noticing that one can obtain symmetric-conjugate methods from palindromic schemes and vice versa. Thus, in particular, by composing the palindromic scheme (30) with its complex conjugate we can form a symmetric-conjugate splitting method with 8 stages and $a_j \in \mathbb{R}$, $b_j \in \mathbb{C}$:

$$\Xi^{[4]}_{SC,r}(\tau) = \Psi^{[4]}_{P,r}(\tau/2)\, \overline{\Psi}^{[4]}_{P,r}(\tau/2), \tag{33}$$

whereas doing the same with the 3rd-order symmetric-conjugate method (28) results in the 4th-order palindromic scheme with 6 stages and $a_j \in \mathbb{R}$, $b_j \in \mathbb{C}$:

$$\Xi^{[4]}_{P,r}(\tau) = \Psi^{[3]}_{SC,r}(\tau/2)\, \overline{\Psi}^{[3]}_{SC,r}(\tau/2). \tag{34}$$

This is possible because the adjoint of $(\Psi^{[3]}_{SC,r}(\tau))^*$ verifies

$$(\Psi^{[3]}_{SC,r}(\tau))^* = \overline{\Psi}^{[3]}_{SC,r}(\tau).$$

In our numerical experiments we shall also use for comparison one of the best 4th-order splitting methods with real coefficients designed specifically for systems verifying (26). It reads

$$\Psi^{[4]}_{RKN}(\tau) = (b_1, a_1, b_2, a_2, b_3, a_3, b_4, a_3, b_3, a_2, b_2, a_1, b_1) \tag{35}$$

and the coefficients can be found in [8]. The scheme has three additional parameters that are used to minimize error terms at higher orders, and provides by construction unitary approximations.

5. **Numerical experiments.** We next report on some numerical tests we have carried out with the splitting methods presented in section 4 applied to the Scrödinger equation in one dimension. Since many different schemes are tested and compared, it is convenient to classify them into the following categories:

- symmetric-conjugate methods with $a_j \in \mathbb{R}$, $b_j \in \mathbb{C}$
  - Order 3: $\Psi^{[3]}_{SC,r}$, Eq. (28);
  - Order 4: $\Psi^{[4]}_{SC,r}$, Eq. (32);
- symmetric-conjugate with $a_j \in \mathbb{C}$, $b_j \in \mathbb{C}$: method $\Psi^{[3]}_{SC,c}$, Eq. (29), order 3;
- palindromic with $a_j \in \mathbb{R}$, $b_j \in \mathbb{C}$: method $\Psi^{[4]}_{P,r}$, Eq. (30), order 4;
- palindromic with $a_j \in \mathbb{C}$, $b_j \in \mathbb{C}$: method $\Psi^{[4]}_{P,c}$, Eq. (31), order 4;

For completeness, we also consider the following schemes of order 4 with $a_j \in \mathbb{R}$, $b_j \in \mathbb{C}$:

- symmetric-conjugate obtained from a palindromic method: $\Xi^{[4]}_{SC,r}$, Eq. (33);
- palindromic obtained from a symmetric-conjugate method: $\Xi^{[4]}_{P,r}$, Eq. (34).

Quartic potential. As the first example we take the quartic oscillator

$$V(x) = -\frac{1}{2}x^2 + \frac{1}{20}x^4 \tag{36}$$

and the initial condition $\psi_0(x) = \sigma\, \mathrm{e}^{-x^2/2}$, where σ is a normalization constant. As usual, and since the exact solution decays rapidly, we truncate the infinite spatial domain to the periodic domain $[-L, L]$, provided L is sufficiently large and use Fourier spectral methods. We take $L = 8$ and set up a uniform grid on the interval with $N = 128$ subdivisions. Finally, we apply the different schemes to integrate in time the resulting equation (23) in the interval $t \in [0, t_f]$, with $t_f = 8000$. As in the case of the example in SU(2), we check the behavior of each scheme with respect to unitarity by computing $|\|u_{\mathrm{app}}(t)\| - 1|$ along the integration, where $u_{\mathrm{app}}(t)$ denotes the numerical approximation obtained by each method.

In addition, we also compute the expected value of the energy, $u^*_{\mathrm{app}}(t) \cdot H u_{\mathrm{app}}(t)$ and measure the error as the difference with respect to the exact value:

$$\text{energy error:} \quad |u^*_{\mathrm{app}}(t) \cdot (H u_{\mathrm{app}}(t)) - u^*_0 \cdot (H u_0)|. \tag{37}$$

In each case, the time step is adjusted so that the number of FFTs (and their inverses) are the same for all methods (specifically, 1572864), so that the computational cost of all schemes is similar.

Figure 3 shows the corresponding results obtained by palindromic schemes with the coefficients a_j real, $\Psi^{[4]}_{P,r}$, and a_j complex, $\Psi^{[4]}_{P,c}$, together with the symmetric-conjugate method $\Psi^{[3]}_{SC,c}$ with $a_j \in \mathbb{C}$. We notice that the qualitative behavior of all of them is similar: after some point, depending on the particular step size, the unitarity is lost and the error in energy grows rapidly.

We notice here the same type of behavior observed in the case of the group SU(2): palindromic schemes with both real and complex coefficients a_j are unable to preserve unitarity. On the other hand, symmetric-conjugate schemes with $a_j \in \mathbb{C}$

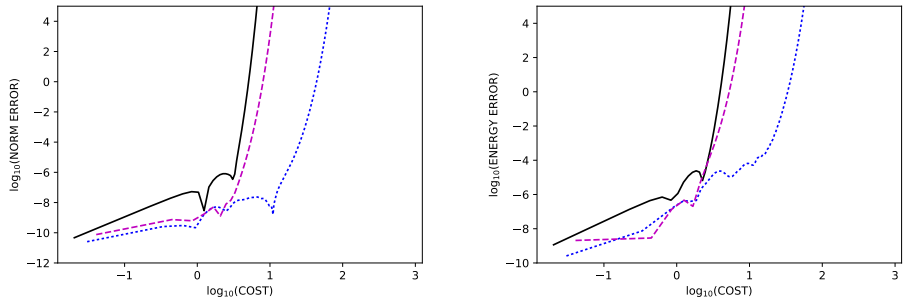

FIGURE 3. Error in norm of the approximate solution (left) and error in energy (37) (right) for the quartic potential (36) obtained by the palindromic schemes $\Psi^{[4]}_{P,r}$ (magenta, dashed line), $\Psi^{[4]}_{P,c}$ (blue dotted line) and the symmetric-conjugate method $\Psi^{[3]}_{SC,c}$ (black solid line) along the integration interval. The step size is chosen so that all methods have the same computational cost.

lead also to unbounded errors, according with the comments formulated at the beginning of section 4.

We collect in Figure 4 the corresponding results achieved by the palindromic method $\Xi^{[4]}_{P,r}$ (blue dotted line), and the symmetric-conjugate schemes $\Psi^{[3]}_{SC,r}$ (black solid line) and $\Xi^{[4]}_{SC,r}$ (magenta dashed line), all of them with real parameters a_j. It is worth noticing that both the norm of the solution and the expected value of the energy are preserved for very long times by symmetric-conjugate methods with $a_j \in \mathbb{R}$, and this happens even if the method is obtained by composing a palindromic scheme (with a poor behavior) with its complex conjugate. By contrast, a symmetric-conjugate method looses its good preservation properties when composed to form a palindromic scheme, even if all a_j are real.

We have carried out the same experiment, but with the roles of T and V interchanged. In other words, the complex coefficients b_j are now multiplying the discretized Laplacian. In that case, the errors obtained by all the previous schemes grow unbounded. This indicates that, at least for this example, one needs both symmetric-conjugate schemes and real coefficients multiplying the Laplacian to get bounded errors in the preservation of unitarity and energy.

Pöschl–Teller potential. The next set of simulations is carried out with the well known one-dimensional Pöschl–Teller potential,

$$V(x) = -\frac{\lambda(\lambda+1)}{2}\operatorname{sech}^2(x), \tag{38}$$

with $\lambda(\lambda+1) = 10$. It has been used in polyatomic molecular simulations and admits an analytic treatment [12]. We take again as initial condition $\psi_0(x) = \sigma\, \mathrm{e}^{-x^2/2}$, with σ a normalizing constant, then apply Fourier spectral methods on the interval $x \in [-8, 8]$ and integrate until the final time $t_f = 8000$ with the previous numerical splitting methods. For this potential we take $N = 512$ subdivisions of the space interval to better visualize the behavior of the different methods. Figure 5 is the analogous of Fig. 3, and only displays the results obtained by $\Psi^{[3]}_{SC,c}$ (black solid

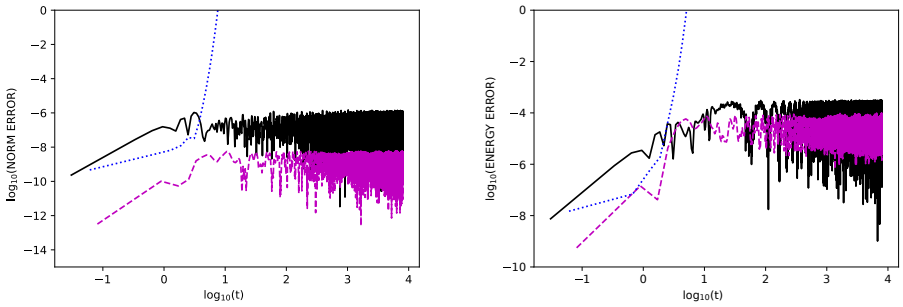

FIGURE 4. Error in norm of the approximate solution (left) and error in energy (37) (right) for the quartic potential (36) obtained by the palindromic scheme $\Xi^{[4]}_{P,r}$ (blue dotted line), and the symmetric-conjugate schemes $\Psi^{[3]}_{SC,r}$ (black solid line) and $\Xi^{[4]}_{SC,r}$ (magenta dashed line) along the integration interval. The step size is chosen so that all methods have the same computational cost.

line) and $\Psi^{[4]}_{P,c}$ (blue dotted line), since the output corresponding to $\Psi^{[4]}_{P,r}$ is out of the scale (the errors are greater than 10^{87}). On the other hand, Figure 6 shows the same pattern as Figure 4: only symmetric-conjugate schemes with $a_j \in \mathbb{R}$ provide bounded errors in the norm and in the energy of the solution.

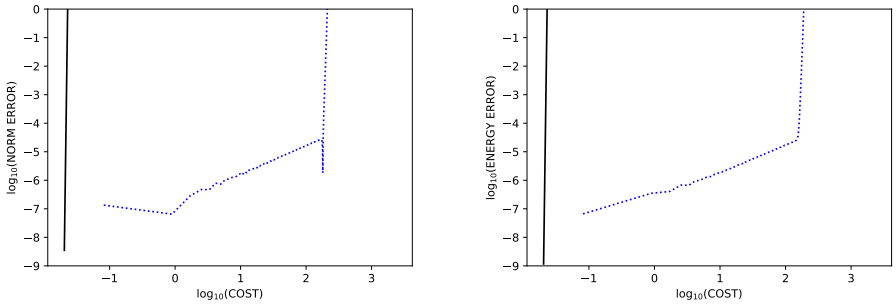

FIGURE 5. Error in norm of the approximate solution (left) and error in energy (37) (right) for the Pöschl–Teller potential (38) obtained by the palindromic scheme $\Psi^{[4]}_{P,c}$ (blue dotted line) and the symmetric-conjugate method $\Psi^{[3]}_{SC,c}$ (black solid line) along the integration interval. The result achieved by $\Psi^{[4]}_{P,r}$ is out of the scale.

Next, we take a shorter final time $t_f = 100$ and compute the maximum error in the energy along the time interval for several step sizes $h = \Delta t$ and integration schemes. The corresponding results are displayed in a log-log diagrama in Figure 7 (left). The order of each method is clearly visible, as well as the values of h where instabilities take place. Finally, in Figure 7 (right) we depict the same results but in terms of the computational cost as measured by the number of FFTs necessary to carry out the calculations. Notice that, for this range of times, the efficiency

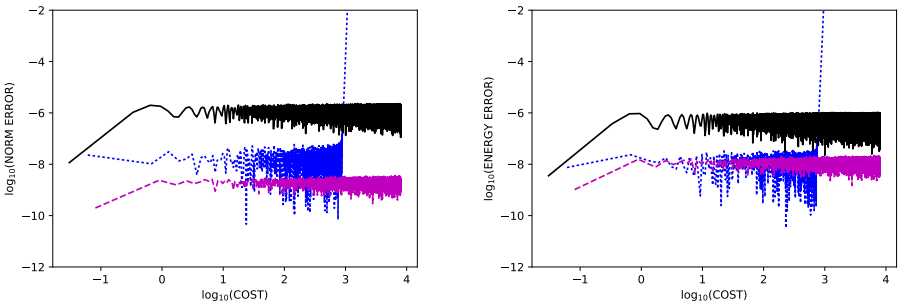

FIGURE 6. Error in norm of the approximate solution (left) and error in energy (37) (right) for the Pöschl–Teller potential (38) obtained by the palindromic scheme $\Xi^{[4]}_{P,r}$ (blue dotted line), and the symmetric-conjugate schemes $\Psi^{[3]}_{SC,r}$ (black solid line) and $\Xi^{[4]}_{SC,r}$ (magenta dashed line) along the integration interval.

of the 4th-order symmetric-conjugate methods is not far away from the optimized scheme (35) that takes into account the special property (26).

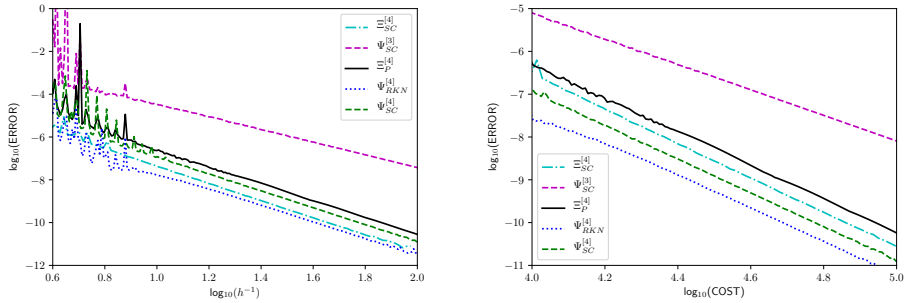

FIGURE 7. Maximum of error in the expected value of the energy in the interval $t \in [0, 100]$ as a function of the time step (left) and the computational cost (number of FFTs, right) for several splitting schemes. Pöschl–Teller potential.

6. **Concluding remarks.** Splitting and composition methods with complex coefficients have shown to be an appropriate tool in the numerical time integration of differential equations of parabolic type, when one or more pieces of the equations are only defined in semi-groups and the aim is to get high accuracy. Since it is possible to design methods of this class with positive real part, one is thus able to circumvent the existing order barrier for methods with real coefficients. In addition, these methods involve smaller truncation errors than their real counterparts and also exhibit relatively large stability thresholds. On the other hand, their computational cost notably increases, due to the use of complex arithmetic.

More recently, it has been shown that the particular class of symmetric-conjugate methods still exhibits remarkable preservation properties when applied to differential equations defined by real vector fields and the solution is projected on the real

axis at each integration step. Here we have extended the analysis to problems evolving in the SU(2) and more generally to the numerical integration of the Schrödinger equation, where preservation of unitarity is a physical requirement. In the former case we have shown explicitly that symmetric-conjugate splitting methods are indeed conjugate to unitary methods for sufficiently small time step sizes, and thus there is not a secular component in the unitarity error propagation.

With respect to the Schrödinger equation, the examples we collect here indicate that methods of this class (with real coefficients a_j) could safely be applied just as other schemes involving only real coefficients for sufficiently small step sizes, although a general theoretical analysis similar to the one developed here for problems defined in SU(2) is lacking at present. Such analysis is clearly more involved, since one has to take into account the effect of the space discretization, the possible introduction of artificial cut-off bounds for unbounded potentials, etc. In this sense, this paper should be considered as a preliminary step for such analysis. In any case, we should remark that the use of methods with complex coefficients in this setting does not imply any extra computational cost, since the problem has to be treated in the complex domain anyway. Our results show that even some of the simplest methods within this class provide efficiencies close to the best standard splitting schemes specifically designed for the integration of the Schrödinger equation. Although we have limited ourselves here to methods of order 3 and 4, it is clear that higher order integrators can also be designed, just by solving the corresponding order conditions [6, 15], and more efficient schemes can be obtained by taking into account property (26) and the processing technique. It is also worth noticing that, in contrast with the time integration of parabolic differential equations, here schemes with real and *negative* coefficients a_j still provide unitary approximations, and so more efficient schemes with $a_j < 0$ and $b_j \in \mathbb{C}$ might be possible. All these issues will be treated in a forthcoming paper.

REFERENCES

[1] A. Bandrauk, E. Dehghanian and H. Lu, Complex integration steps in decomposition of quantum exponential evolution operators, *Chem. Phys. Lett.*, **419** (2006), 346–350.

[2] S. Blanes and F. Casas, On the necessity of negative coefficients for operator splitting schemes of order higher than two, *Appl. Numer. Math.*, **54** (2005), 23–37.

[3] S. Blanes and F. Casas, *A Concise Introduction to Geometric Numerical Integration*, Monographs and Research Notes in Mathematics. CRC Press, Boca Raton, FL, 2016.

[4] S. Blanes, F. Casas, P. Chartier and A. Escorihuela-Tomàs, On symmetric-conjugate composition methods in the numerical integration of differential equations, `arXiv:2101.04100` (to appear in *Math. Comput.*).

[5] S. Blanes, F. Casas, P. Chartier and A. Murua, Optimized high-order splitting methods for some classes of parabolic equations, *Math. Comput.*, **82** (2013), 1559–1576.

[6] S. Blanes, F. Casas and A. Murua, Splitting and composition methods in the numerical integration of differential equations, *Bol. Soc. Esp. Mat. Apl.*, **45** (2008), 89–145.

[7] S. Blanes, F. Casas and A. Murua, Splitting methods with complex coefficients, *Bol. Soc. Esp. Mat. Apl.*, **50** (2010), 47–60.

[8] S. Blanes and P. Moan, Practical symplectic partitioned Runge–Kutta and Runge–Kutta–Nyström methods, *J. Comput. Appl. Math.*, **142** (2002), 313–330.

[9] F. Casas, P. Chartier, A. Escorihuela-Tomàs and Y. Zhang, Compositions of pseudo-symmetric integrators with complex coefficients for the numerical integration of differential equations, *J. Comput. Appl. Math.*, **381** (2021), 113006.

[10] F. Castella, P. Chartier, S. Descombes and G. Vilmart, Splitting methods with complex times for parabolic equations, *BIT Numer. Math.*, **49** (2009), 487–508.

[11] J. Chambers, Symplectic integrators with complex time steps, *Astron. J.*, **126** (2003), 1119–1126.

[12] S. Flügge, *Practical Quantum Mechanics*, Springer, 1971.
[13] A. Galindo and P. Pascual, *Quantum Mechanics. I.*, Texts and Monographs in Physics. Springer-Verlag, Berlin, 1990.
[14] F. Goth, Higher order auxiliary field quantum Monte Carlo methods, arXiv:2009.04491.
[15] E. Hairer, C. Lubich and G. Wanner, *Geometric Numerical Integration. Structure-Preserving Algorithms for Ordinary Differential Equations*, 2^{nd} edition, Springer-Verlag, 2006.
[16] E. Hansen and A. Ostermann, Exponential splitting for unbounded operators, *Math. Comput.*, **78** (2009), 1485–1496.
[17] E. Hansen and A. Ostermann, High order splitting methods for analytic semigroups exist, *BIT Numer. Math.*, **49** (2009), 527–542.
[18] C. Lubich, *From Quantum to Classical Molecular Dynamics: Reduced Models and Numerical Analysis*, European Mathematical Society, 2008.
[19] R. McLachlan and R. Quispel, Splitting methods, *Acta Numer.*, **11** (2002), 341–434.
[20] T. Prosen and I. Pizorn, High order non-unitary split-step decomposition of unitary operators, *J. Phys. A: Math. Gen.*, **39** (2006), 5957–5964.
[21] Q. Sheng, Solving partial differential equations by exponential splitting, *IMA J. Numer. Anal.*, **9** (1989), 199-212.
[22] M. Suzuki, Fractal decomposition of exponential operators with applications to many-body theories and Monte Carlo simulations, *Phys. Lett. A*, **146** (1990), 319–323.
[23] M. Suzuki, General theory of fractal path integrals with applications to many-body theories and statistical physics, *J. Math. Phys.*, **32** (1991), 400–407.

Received March 2021; revised August 2021; early access December 2021.

E-mail address: serblaza@imm.upv.es
E-mail address: Fernando.Casas@mat.uji.es
E-mail address: alescori@uji.es